11th World Congress on Structural and Multidisciplinary Optimization
7th - 12th, June 2015, Sydney Australia

A Novative Optimal Shape Design Based on an Isogeometric Approach: Application to Optimization of Surface Shapes With Discontinuous Curvature.

Sarah Julisson[1,2,3], Christian Fourcade[2], Paul de Nazelle[3], Laurent Dumas[1]

[1] University of Versailles Saint-Quentin-en-Yvelines, Versailles, France, laurent.dumas@uvsq.fr
[2] Renault S.A.S, Guyancourt, France, christian.fourcade@renault.com
[3] IRT SystemX, Palaiseau, France, sarah.julisson@irt-systemx.fr, paul.denazelle@irt-systemx.fr

1. Abstract
When designing complex structures, optimization can play a major role. The most common procedure uses finite element analysis conducted on a mesh of the shape. Since the mesh is an approximation of the structure geometry, the quality of the simulations and consequently the optimization results are often downgraded. In this paper, we propose a computation method using the exact shape geometry for multi-shells structures. This method is based on isogeometric approach and allows to get better computation and optimization results.

2. Keywords: Isogeometry, Thin Shell, Shell Junctions, Shape Optimization.

3. Introduction
In order to conceive better products, industrial projects use more and more optimization methods during the numerical design process. The common work-flow relies on different steps. Each of these steps requires a particular expertise. In the case of automotive industry, designers create a parameterized shape, known as the CAD model, then engineers mesh it and run simulations using finite elements analysis to carry out the shape optimization [12]. This standard process raises several limitations such as: the design time, the computational cost and one of the most important, the return to a CAD model from a mesh after computation, which can corrupt the optimization expectations. To offset these limitations, some methods like the isogeometric approach have been proposed. The isogeometric consists on running computations directly on the shape by using the exact geometry of the shape to perform the finite elements analysis[6], [7]. Thereby, the difficulty of the CAD return disappears since the optimization is conducted on the geometry described by the CAD model. In this paper, we propose a method based on the isogeometric approach for surface shape using deep shell models. As they enable high curvature variations, deep shells represent a great interest in the automotive industry and for shape optimization. The technique we present uses shape functions based on Bézier's patches of the CAD model. Since complex structures are designed with the help of multiple CAD patches, we consider each patch as a Koiter's shell and we ensure the connections between patches with shell junctions. This process enables to carry out optimization on shape with discontinuous curvature. In the first part of this paper, we recall the Koiter's shell model, deal with shell junctions in the next and finally we present the results of an optimization test case.

4. Koiter's shell linear model
Thin shells are used as components in many industrial structures and thus are a real concern in numerical simulation. In this paper, we will use the Einstein's summation convention. Both Greek indices or exponents take their values in $\{1,2\}$ while Roman are in $\{1,2,3\}$.

4.1. Description of a thin shell geometry
Let Ω be a open subset in a plane $\mathscr{E}^2$,the euclidean space, with a boundary noted Γ. The middle surface $\mathscr{S}$ of a shell is defined as the image in $\mathscr{E}^3$ of $\overline{\Omega}$ by a mapping $\vec{\phi} \in (\mathscr{C}^3(\overline{\Omega}))^3$:

$$\vec{\phi} : (\xi^1, \xi^2) \in \Omega \subset \mathscr{E}^2 \rightarrow \vec{\phi}(\xi^1, \xi^2) \in \mathscr{S} \subset \mathscr{E}^3 \tag{1}$$

ϕ is called the shape function and Ω the reference domain, which is independent from the shape. The mechanical equations are formulated on the reference domain in curvilinear coordinates. In the interest of formulating the mechanical equations, we recall some differential geometry entities. We define the two linearly independent vectors $\vec{a}_\alpha = \vec{\phi}_{,\alpha} = \partial\phi/\partial\xi^\alpha, \quad \alpha = 1,2$ for all points $\xi = (\xi^1, \xi^2) \in \overline{\Omega}$. The (a_α) vectors define the tangent plane to the middle surface. With the unit normal vector $\vec{a}_3 = \vec{a}_1 \wedge \vec{a}_2 / |\vec{a}_1 \wedge \vec{a}_2|$, they constitute the covariant basis. Associated to the covariant basis, the contravariant basis is defined through the relation $\vec{a}^\alpha . \vec{a}_\beta = \delta^\alpha_\beta$ where

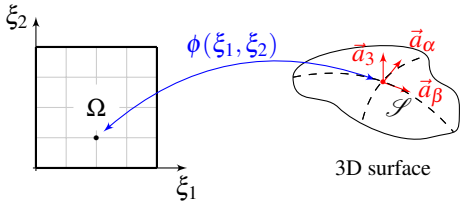

Figure 1: Definition of the middle surface

δ^α_β is the Kronecker's symbol. The first fundamental covariant form is given by $a_{\alpha\beta} = a_{\beta\alpha} = \vec{a}_\alpha.\vec{a}_\beta$ and the second by $b_{\alpha\beta} = b_{\beta\alpha} = -\vec{a}_\alpha.\vec{a}_{3,\beta} = \vec{a}_3.\vec{a}_{\alpha,\beta} = \vec{a}_3.\vec{a}_{\beta,\alpha}$. The mixed components of the second fundamental form are defined by $b^\beta_\alpha = a^{\beta\lambda}b_{\lambda\alpha}$ with $a^{\alpha\beta} = \vec{a}^\alpha.\vec{a}^\beta$. Finally, in order to compute the basis vector derivative, $\vec{a}_{\alpha,\beta} = \Gamma^\gamma_{\alpha\beta}\vec{a}_\gamma + b_{\alpha\beta}\vec{a}_3$; $\vec{a}^\alpha_{,\beta} = -\Gamma^\alpha_{\beta\lambda} + b^\alpha_\beta\vec{a}_3$; $\vec{a}_{3,\alpha} = \vec{a}^3_{,\alpha} = -b^\gamma_\alpha\vec{a}_\gamma$. Christoffel's symbols are also used to compute the covariant derivative of surface tensors: $T_{\alpha|\gamma} = T_{\alpha,\gamma} - \Gamma^\lambda_{\alpha\gamma}T^\lambda$; $T^\alpha|_\gamma = T^\alpha_{,\gamma} + \Gamma^\lambda_{\lambda\gamma}T^\lambda$. The origin and the relations between all these entities are detailed in [6].

4.2. Koiter's shell model

The Koiter's thin shell model was introduced by W. T. Koiter in 1966. The linear model relies on the Kirchhoff-Love assumptions: straight lines normal to the middle surface remain normal to the middle surface after deformation and the stresses remain plane and parallel to the tangent plane of the middle surface. We assume that the shell is clamped along a part Γ_0 of its boundary and that it is loaded on its complementary part Γ_1 by a distributed force $\vec{N}$ and a distributed moment $\vec{M}$. We also suppose that $\vec{p}$ is the external loads referred to the middle surface and $\vec{\psi}(\vec{v})$ is the infinitesimal rotation vector such as $\vec{\psi}(\vec{v}) = \varepsilon^{\lambda\beta}(v_{3,\beta} + b^\alpha_\beta v_\alpha)\vec{a}_\lambda + \frac{1}{2}\varepsilon^{\lambda\beta}v_{\beta|\lambda}\vec{a}_3$. The variational formulation of Koiter's linear model is

$$Find\ \vec{u} \in \vec{V}\ such\ as\ a(\vec{u},\vec{v}) = f(\vec{v}), \quad \forall \vec{v} \in \vec{V} \tag{2}$$

where

$$a(\vec{u},\vec{v}) = \int_\Omega eE^{\alpha\beta\lambda\mu}\left[\gamma_{\alpha\beta}(\vec{u})\gamma_{\lambda\mu}(\vec{v}) + \frac{e^2}{12}\rho_{\alpha\beta}(\vec{u})\rho_{\lambda\mu}(\vec{v})\right]\sqrt{a}d\xi^1 d\xi^2 \tag{3}$$

$$f(\vec{v}) = \int_\Omega \vec{p}\vec{v}\sqrt{a}d\xi^1 d\xi^2 + \int_{\Gamma_1}\vec{N}\vec{v} + \vec{M}\vec{\psi}(\vec{v})ds \tag{4}$$

and

$$\vec{V} = \left\{\vec{v} = (v_\alpha, v_3) \in ((H^1(\Omega))^2 \times H^2(\Omega));\ \vec{v}|_{\Gamma_0} = \vec{0},\ \left.\frac{\partial v_3}{\partial n}\right|_{\Gamma_0} = 0\right\} \tag{5}$$

with $\vec{u} = (u_1, u_2, u_3)$ the displacement of the middle surface, e the shell thickness, $\sqrt{a} = |\vec{a}_1 \wedge \vec{a}_2|$, $E^{\alpha\beta\lambda\gamma}$ the elastic modulus tensor for plane stresses, $\gamma_{\alpha\beta}(\vec{u})$ the middle surface strain tensor, and $\rho_{\alpha\beta}(\vec{u})$ the modified change of curvature tensor. The expression of these tensors are given by: $E^{\alpha\beta\lambda\mu} = \frac{E}{2(1+\nu)}\left[a^{\lambda\mu}a^{\beta\mu} + a^{\alpha\mu}a^{\beta\lambda} + \frac{2\nu}{1-\nu}a^{\alpha\beta}a^{\lambda\mu}\right]$, $\gamma_{\alpha\beta}(\vec{u}) = \frac{1}{2}\left(u_{\alpha|\beta} + u_{\beta|\alpha}\right) - b_{\alpha\beta}u_3$, and $\rho_{\alpha\beta}(\vec{u}) = -(u_{3|\alpha\beta} - b^\lambda_\alpha b_{\lambda\beta}u_3 + b^\lambda_{\alpha|\beta}u_\lambda + b^\lambda_\alpha u_{\lambda|\beta} + b^\lambda_\beta u_{\lambda|\alpha})$ where E is Young's modulus ans ν is Poisson's ratio.

Complex structures are made of multiple shells. To conduct satisfying simulations, each shell must have a good approximation as well as the description of their junctions.

5. Shells junction

5.1. Description of the shells junction problem

In the case of a structure composed of shells connected with $\mathscr{C}^1$ geometric continuity, the equality of the displacement from either side of a junction may be a sufficient condition to ensure the quality of the simulation. However, some constructions like the body frame of a car body are assemblies of several shells with $\mathscr{C}^0$ geometric continuity. In order to treat these parts, we propose to implement the Koiter's shells junction equation described in [2] and [3]. Let $\mathscr{S}$ and $\tilde{\mathscr{S}}$ be two middle surfaces of two shells sharing a common boundary, known as the hinge Γ. $\mathscr{S}$ and $\tilde{\mathscr{S}}$ are the images of reference domains Ω and $\tilde{\Omega}$ by the mappings $\vec{\phi}$ and $\tilde{\vec{\phi}}$. We suppose that $\mathscr{S}$, respectively $\tilde{\mathscr{S}}$, is clamped along a part $\partial\mathscr{S}_0$, respectively $\partial\tilde{\mathscr{S}}_0$, and loaded along a part $\partial\mathscr{S}_1$, respectively $\partial\tilde{\mathscr{S}}_1$. Let $\vec{p}$, respectively $\tilde{\vec{p}}$, be the external load to the middle surface $\mathscr{S}$, respectively $\tilde{\mathscr{S}}$, $\vec{N}$ (respectively $\tilde{\vec{N}}$), the distributed force

on $\partial\mathscr{S}_1$, respectively $\partial\tilde{\mathscr{S}}_1$, and $\vec{M}$ respectively $\vec{\tilde{M}}$ the distributed moment. We note $\gamma = \phi^{-1}(\Gamma)$ and $\tilde{\gamma} = \tilde{\phi}^{-1}(\tilde{\Gamma})$. The figure 2 shows the problem configuration. The action-reaction principle enforces the transmission of stresses.

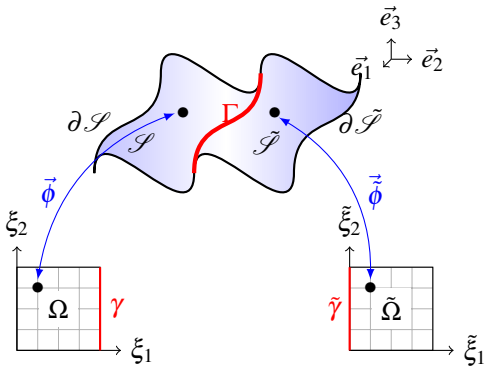

Figure 2: Junction between two shells

Therefore, $\vec{N}(P) = \vec{\tilde{N}}(P)$ and $\vec{M}(P) = \vec{\tilde{M}}(P)$. In [2] and [3], two types of hinge behaviour are considered:

- the rigid behaviour for which the continuity of the displacements and the continuity of the tangential rotations along the hinge Γ are ensured: $\vec{u}(P) = \vec{\tilde{u}}(P) \quad (\vec{\psi}.\vec{t})(P) = (\vec{\tilde{\psi}}.\vec{t})(P) = (\vec{t}.\vec{\tilde{t}})(\vec{\tilde{\psi}}.\vec{\tilde{t}})(P) \quad \forall P \in \Gamma$
- the elastic behaviour for which only the continuity of the displacements is ensured: $\vec{u}(P) = \vec{\tilde{u}}(P) \quad M_n(P) = k[(\vec{\psi} - \vec{\tilde{\psi}}).\vec{t}](P), \quad \forall P \in \Gamma$. The tangential component of moment is proportional to the jump of the tangential components of the rotations along the hinge. The coefficient k represents the elastic stiffness along the hinge.

$\vec{\psi}$ being the infinitesimal rotation vector and $\vec{t}$, respectively $\vec{\tilde{t}}$, the tangent vector to Γ in the tangent plane to $\mathscr{S}$, respectively $\tilde{\mathscr{S}}$. We also introduce the normal vector $\vec{n}$, respectively $\vec{\tilde{n}}$, to the boundary Γ in the tangent plane to $\mathscr{S}$, respectively $\tilde{\mathscr{S}}$.
The variational formulations of the junction problems are determined by summing the Koiter's formulation on each shell and applying the relations expressed above.

5.2. Variational formulations
The variational formulation for a junction problem with an elastic hinge is:

$$\textit{Find } (\vec{u},\vec{\tilde{u}}) \in W_{elas} \textit{ such as } a[(\vec{u},\vec{\tilde{u}}),(\vec{v},\vec{\tilde{v}})] + kb[(\vec{u},\vec{\tilde{u}}),(\vec{v},\vec{\tilde{v}})] = l(\vec{v},\vec{\tilde{v}}) \quad \forall (\vec{v},\vec{\tilde{v}}) \in W_{elas} \tag{6}$$

where

$$W_{elas} = \{(\vec{v},\vec{\tilde{v}}) \in \vec{V} \times \vec{\tilde{V}},\ \vec{v} = \vec{\tilde{v}} \textit{ on } \gamma\} \tag{7}$$

and

$$\left\{ \begin{array}{l} a[(\vec{u},\vec{\tilde{u}}),(\vec{v},\vec{\tilde{v}})] = \displaystyle\int_\Omega eE^{\alpha\beta\lambda\mu}\left[\gamma_{\alpha\beta}(\vec{u})\gamma_{\lambda\mu}(\vec{v}) + \frac{e^2}{12}\rho_{\alpha\beta}(\vec{u})\rho_{\lambda\mu}(\vec{v})\right]\sqrt{a}d\xi^1 d\xi^2 + \\ \qquad\qquad \displaystyle\int_{\tilde{\Omega}} \tilde{e}\tilde{E}^{\alpha\beta\lambda\mu}\left[\tilde{\gamma}_{\alpha\beta}(\vec{\tilde{u}})\tilde{\gamma}_{\lambda\mu}(\vec{\tilde{v}}) + \frac{\tilde{e}^2}{12}\tilde{\rho}_{\alpha\beta}(\vec{\tilde{u}})\tilde{\rho}_{\lambda\mu}(\vec{\tilde{v}})\right]\sqrt{\tilde{a}}d\tilde{\xi}^1 d\tilde{\xi}^2 \end{array} \right. \tag{8}$$

$$b[(\vec{u},\vec{\tilde{u}}),(\vec{v},\vec{\tilde{v}})] = \int_\gamma [n^\beta(u_{3,\beta} + b^\alpha_\beta u_\alpha) - \tilde{n}^\beta(\vec{t}.\vec{\tilde{t}})(\tilde{u}_{3,\beta} + \tilde{b}^\alpha_\beta \tilde{u}_\alpha)][n^\beta(v_{3,\beta} + b^\alpha_\beta v_\alpha) - \tilde{n}^\beta(\vec{t}.\vec{\tilde{t}})(\tilde{v}_{3,\beta} + \tilde{b}^\alpha_\beta \tilde{v}_\alpha)]d\gamma \tag{9}$$

$$l(\vec{v},\vec{\tilde{v}}) = \int_\Omega \vec{p}\vec{v}\sqrt{a}d\xi^1 d\xi^2 + \int_{\partial\Omega_1} \vec{N}\vec{v} + \vec{M}\vec{\psi}(\vec{v})ds + \int_{\tilde{\Omega}} \vec{\tilde{p}}\vec{\tilde{v}}\sqrt{\tilde{a}}d\tilde{\xi}^1 d\tilde{\xi}^2 + \int_{\partial\tilde{\Omega}_1} \vec{\tilde{N}}\vec{\tilde{v}} + \vec{M}\vec{\tilde{\psi}}(\vec{\tilde{v}})d\tilde{s} \tag{10}$$

The variational formulation for a junction problem with a rigid hinge is given by:

$$\textit{Find } (\vec{u},\vec{\tilde{u}}) \in W_{rig} \textit{ such as } a[(\vec{u},\vec{\tilde{u}}),(\vec{v},\vec{\tilde{v}})] = l(\vec{v},\vec{\tilde{v}}) \quad \forall (\vec{v},\vec{\tilde{v}}) \in W_{rig} \tag{11}$$

where:

$$W_{rig} = \{(\vec{v},\vec{\tilde{v}}) \in \vec{V} \times \vec{\tilde{V}},\ \vec{v} = \vec{\tilde{v}} \textit{ on } \gamma\ ;\ n_\beta(v_{3,\beta} + b^\alpha_\beta v_\alpha) - (\vec{t}.\vec{\tilde{t}})\tilde{n}_\beta(\tilde{v}_{3,\beta} + \tilde{b}^\alpha_\beta \tilde{v}_\alpha) = 0 \textit{ on } \gamma\} \tag{12}$$

and a and l correspond to (8) and (10).
The proofs of these results are presented in [3]. Each of these problems admits a unique solution. What is more, the solution of elastic hinge problem converges strongly to the solution of the rigid hinge problem when k tends to infinity.

6. Application of the method in an optimization process

As explained previously, the interest in using an isogeometric approach is the idea of working on the exact geometry of the shape. This approach can be useful in a shape optimization work-flow when at the end of the optimization the return to a CAD model is immediate. Some optimization results using the same method for one patch are presented in [10]. In this paragraph, we will combine our method with an optimization problem and present the first results.

6.1. The shape function

The shape function $\vec{\phi}$ is the link between the reference domain in dimension 2, Ω, and the surface in dimension 3. In order to describe an exact geometric model, CAD model patches are used to define the shape functions. Several types of patches can be used in CAD modelling. Bézier's surfaces, B-Spline surfaces or NURBS constitute some of them. The definition and properties of these surfaces are detailed in [11]. In our case, Bézier's surfaces are the components of the shape functions. A Bézier's surface is defined as a tensor product of two Bézier's curves. The expression of a Bézier's curve of degree n is given by:

$$\mathscr{C}(u) = \sum_{i=0}^{n} B_{i,n}(u) P_i \quad 0 \leq u \leq 1 \tag{13}$$

where the basis functions $\{B_{i,n}(u)\} = \frac{n!}{i!(n-i)!} u^i (1-u)^{n-i}$ are Bernstein polynomials of degree n. The coefficient P_i are called the control points or poles and are the geometric coefficient that tune the curve. Thus, a Bézier's surface of degree n and m can be expressed by:

$$\mathscr{B}(u,v) = \sum_{i=0}^{n} \sum_{j=0}^{m} B_{i,n}(u) B_{j,m}(v) P_{i,j} \quad 0 \leq u,v \leq 1 \tag{14}$$

CAD models are composed of multiple patches. In our approach, we consider each patch as a shell and ensure the

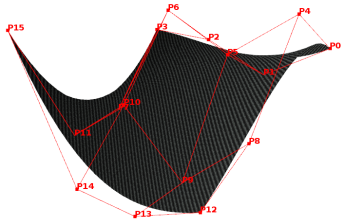

Figure 3: Example of a Bézier surface of degree 3

connection between them with shells junction conditions. As Bézier's surfaces are defined by their control points, these poles will be the optimization's variables. In comparison, for a classical industrial optimization problem, the number optimization variables matches the number of the shape's nodes mesh, which can be significant. By choosing the control points as variables, the dimension of the optimization problem substantially decreases.

6.2. The optimization problem

As a test case, we considered the optimization of the plate shape presented in Figure 4 under a compliance criteria. We supposed that the structure, modeled by two Bézier's patches of degree 5, is supported on its curved edges and subjected to self weight. A shape optimization problem is composed of an objective function $J(\vec{\phi})$ to minimize and a state equation depending on the shape function ϕ, and a space of admissible shapes $\mathscr{G}_{ad}$. In this application, the state equation is given by the equations (6) or (11). The space of admissible shapes is described by the constraints on the control points of the surfaces. The studied optimization problem is:

$$\begin{cases} \min\limits_{\phi \in \mathscr{G}_{ad}} J(\vec{\phi}, \vec{u_p}) \\ subject\ to \quad \{Find\ \vec{u_p} \in W\ such\ as\ a_p(\vec{\phi}, \vec{u_p}, \vec{v_p}) = f_p(\vec{\phi}, \vec{v_p}) \quad \forall \vec{u_p} \in W\} \end{cases} \tag{15}$$

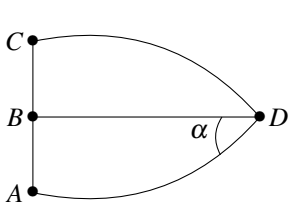

$$AB = BC = 10$$
$$\alpha = 60^o$$
$$e = 0.025$$
$$E = 4.32.10^8$$
$$\nu = 0.0$$

Figure 4: Description of the shape of the test case

where $\vec{u}_p = (\vec{u}, \vec{\tilde{u}})$ and $\vec{v}_p = (\vec{v}, \vec{\tilde{v}})$. The state equation depends on the type of junction. For an elastic hinge $W = W_{elas}$ from (7) and $a_p(\vec{\phi}, \vec{u_p}, \vec{v_p}) = a[(\vec{u}, \vec{\tilde{u}}), (\vec{v}, \vec{\tilde{v}})] + kb[(\vec{u}, \vec{\tilde{u}}), (\vec{v}, \vec{\tilde{v}})]$ from (8) and (9). For a rigid hinge $W = W_{rig}$ from (12) and $a_p(\vec{\phi}, \vec{u_p}, \vec{v_p}) = a[(\vec{u}, \vec{\tilde{u}}), (\vec{v}, \vec{\tilde{v}})]$ from (8). In both configurations, $f_p(\vec{\phi}, \vec{v_p}) = l(\vec{v}, \vec{\tilde{v}})$ with l from (10). Since the optimization criteria is the compliance $J(\vec{\phi}, \vec{u_p}) = \frac{1}{2} a_p(\vec{\phi}, \vec{u_p}, \vec{u_p})$, the space of admissible shapes $\mathscr{G}_{ad}$ depends on the constraints imposed to the shape. Its definition is crucial as it has a direct impact on the existence of a solution to the optimization problem. We have chosen as optimization variables only the z coordinates of the control net. Regarding the constraints, we imposed the equality of the poles located on the hinge and that the area of the optimal shape must be around $\pm 15\%$ of the area of the original surface. The problem (15) admits at least one solution with theses conditions. The algortihm used for the optimization is the Powell's free-derivative algorithm COBYLA.

6.3. Results

The result provided by the algorithm is the shape displayed on Figure 5(b). The compliance has droped by 24% and the area has increased of 12% approximately. The new shape presents more curvatures and thus is more subjected to membrane deformations than bending deformations that stiffen the structure. It has been observed that discontinuous curvature appeared during the optimization especially at the point (D). The implementation of the shell junction allows to carry on computations even with this discontinuity. Those results are encouraging and corroborate the efficiency of the method. The next step in this work will consist in comparing the results with other examples in the litterature [5],[8],[13].

(a) original shape (b) optimized shape

Figure 5: Original shape and optimization result

7. Conclusion

The application showed that the proposed method can be integrated in a shape optimization process with a result given in the form of a CAD model. On the other hand, several shapes could be considered, even shapes with discontinuous curvature. However, as mentionned previously, the definition of the optimization problem can raise some difficulties. Indeed, as in every shape optimization problem, the space of admissible solution must be carefully chosen in order to ensure the existence of a solution. Besides, in the application case, as the optimization variables are control points, the shape constraints must be expressed on the control points, which can be difficult ine some cases.

8. Acknowledgements

This research work has been carried out in the framework of the Technological Research Institute SystemX in collaboration with Renault S.A.S and the University of Versailles Saint-Quentin-Yvelines. It is therefore partially granted with public funds within the scope of the French Program "Investissements d'Avenir".

9. References

[1] G. Allaire, *Conception optimale des structures*, Springer-Verlag, Berlin, 2007.

[2] M. Bernadou, *Méthodes des Éléments Finis Pour les Problèmes de Coques Minces*, Masson, Paris, 1994.

[3] M. Bernadou and A. Cubier, *Numerical Analysis of Junctions Between Thin Shell, Part 1: Continuous Problems*, Research report, INRIA, 1996.

[4] M. Bernadou and A. Cubier, *Numerical Analysis of Junctions Between Thin Shell, Part 2: Approximation by Finite Elements Methods*, Research report, INRIA, 1996.

[5] K. Bletzinger, M. Firl, J. Linhard, and R. Wuchner, Optimal shapes of mechanically motivated surfaces, *Computer Methods in Applied Mechanics and Engineering*, 199(5-8):324 333, 2010. ISSN 0045-7825.

[6] P. G. Ciarlet, *An Introduction to Differential Geometry With Applications to Elasticity*, Springer-Verlag, New York Inc, 2006.

[7] T. J. R. Hughes, J. A. Cottrell and, Y. Bazilevs, *Isogeometric analysis: Toward Integration of CAD and FEA*, Wiley-Blackwell, 2009.

[8] M. C. Delfour and J.-P. Zolésio, *Shapes and Geometries: Metrics, Analysis, Differential Calculus, and Optimization*, SIAM, 2010. ISBN 978-0-898714-89-0.

[9] J. M. Kiendl, *Isogeometric Analysis ans Shape Optimal Design of Shell Structures*, Ph.D Thesis, Technische Universitat Munchen, 2011.

[10] P. de Nazelle, *Paramétrage de formes surfaciques pour l'optimisation*, Ph.D Thesis, Ecole Centrale de Lyon, 2013.

[11] L. Piegl and W. Tiller, *The NURBS Book, Second Edition*, Springer-Verlag, Berlin, 1997.

[12] K. Saitou, K. Izui, S. Nishiwaki and P. Papalambros, A Survey of Structural Optimization in Mechanical Product Development, *Journal of Computing and Information Science in Engineering*,vol. 5, no. 3, pages 214-226, 2005.

[13] J. Sokolowski, *Displacement derivatives in shape optimization of thin shells* Research report, INRIA, 1996.